# Wide-Range Wavelength-Tunable Mode-Locked Fiber Laser Based on Fiber Bragg Grating

Fengqin Huang<sup>1</sup>, Jinhai Si<sup>1\*</sup>, Tao Chen<sup>1</sup>, Lei Hou<sup>2</sup>, Xun Hou<sup>1</sup>

Abstract—We demonstrated a wide-range wavelength-tunable passively mode-locked fiber laser based on the fiber Bragg grating (FBG) fabricated by femtosecond laser as the wavelength selection element. A ring fiber cavity with the nonlinear-optical loop mirror as its saturable absorber was employed for mode-locking operation. The peak wavelength of the fiber laser was 1547.9 nm with a spectral full-width-at-half-maximum of 0.90 nm at room temperature. The pulse duration of the fiber laser was about 2.94 ps closed to the Fourier-limited pulse duration of 2.80 ps by assuming sech² pulse shape. The repetition rate was 860.5 kHz and the pulse peak power was about 56.2 W. The wavelength tuning range of the fiber laser achieved 14.2 nm by varying the FBG temperature from 25  $\,^{\circ}$ C to 1000  $\,^{\circ}$ C.

Index Terms—Fiber Bragg gratings, passively mode-locked fiber lasers, wavelength-tunable fiber lasers.

## I. INTRODUCTION

AVELENGTH-TUNABLE mode-locked (ML) fiber lasers have wide applications in linear optical sampling [1], optical sensing [2], coherent nonlinear-optical microscopy [3], and so on. Many methods have been explored to achieve wavelength tuning in ML fiber lasers, including inserting wavelength selection elements in laser cavity [4]-[11], tuning cavity birefringence [12], [13] or cavity dispersion [14] et al. The common way is to insert wavelength selection elements in laser cavities, such as tunable bandpass filters [4]-[6], Sagnac fiber filters [7], [8], unbalanced Mach-Zehnder interferometers [9], and fiber Bragg gratings (FBGs) [10], [11]. Among them, FBGs have particular merits of small in size and low insertion loss.

Bragg wavelengths of FBGs can be tuned by changing strain [15] or temperature [16]. FBG-based pulsed fiber lasers have achieved wavelength-tunable operation by applying axial-strain to FBGs. Zhou et al. reported a tunable passively Q-switched Erbium-doped fiber laser with an FBG as its

This work was supported in part by the National Key Research and Development Program of China under Grant 2017YFB1104600, in part by Key research and development program of Shaanxi province under Grant 2017ZDXM-GY-120, in part by Fundamental Research Funds for the Central Universities under Grant XJJ2016016. (Corresponding author: Jinhai Si.)

Fengqin Huang, Jinhai Si, Tao Chen, Xun Hou are with the Key Laboratory of Physical Electronics and Devices, Ministry of Education & Shaanxi Key Lab of Information Photonic Technique, School of Electronic science and Engineering, Xi'an Jiaotong University, Xi'an Shaanxi 710049, China (e-mail: hfq4117005070@stu.xjtu.edu.cn; jinhaisi@mail.xjtu.edu.cn; tchen@xjtu.edu.cn; houxun@mail.xjtu.edu.cn).

Lei Hou is with the National Key Laboratory of Photoelectric Technology and Functional Materials (Culture Base), Institute of Photonics and Photon-Technology, Northwest University, Xi'an Shaanxi 710069, China (email: lhou@nwu.edu.cn).

wavelength selection element and its wavelength can be tuned from 1555 to 1560 nm [10]. Litago et al. demonstrated an FBG-based wavelength-tunable ML soliton fiber laser with a wavelength tuning range of over 8.6 nm [11]. Wavelength-tunable fiber lasers have also been realized by changing FBG temperatures [17]-[18]. Wang et al. reported a passively FBG-based ML picosecond Erbium doped fiber laser and the fiber laser achieved a 0.79 nm wavelength tuning range by control FBG temperature [17]. Shen et al. reported a continuous wave (CW) fiber laser based on two high temperature sustainable FBGs which can work up to 400 °C. Its wavelength tuning range was about 6 nm [18]. However, since conventional FBGs fabricated by long-pulse UV lasers will be erased above 400 °C, wavelength tuning ranges of FBG-based fiber lasers are limited by the temperature resistance of FBG.

Compared to those fabricated by long-pulse UV lasers, FBGs fabricated by femtosecond (FS) lasers [19]-[21] have unique advantages of no photosensitivity requirement for the fiber and wonderful thermal stability. Especially, type II FBGs can stably work up to 1000 °C [22], [23]. We have demonstrated a wavelength-tunable CW fiber laser based on a FS laser fabricated type II FBG. Its wavelength tuning range reached 14.3 nm by varying the FBG temperature from 25 °C to 1000 °C [24]. Wavelength-tunable fiber lasers can also be used as strain or temperature sensors. By using ML fiber laser as light source, FBG sensing interrogation method achieved finer wavelength spacing between FBG channels than that using CW light [2]. Hence, ML fiber lasers based on type II FBG are very meaningful for increasing the number of multiplexed FBGs in high temperature sensing.

demonstrate a this paper, we wide-range wavelength-tunable passively ML fiber laser based on the FS laser-inscribed FBG as the wavelength selection element. A ring cavity with the nonlinear-optical loop mirror (NOLM) as its saturable absorber (SA) was employed for mode-locking operation. The peak wavelength of the ML fiber laser was 1547.9 nm with a spectral full-width-at-half-maximum (FWHM) of 0.90 nm at room temperature (25  $^{\circ}$ C). The pulse duration of output pulses was about 2.94 ps by assuming sech<sup>2</sup> pulse shape. The repetition rate and pulse peak power were 860.5 kHz and 56.2 W, respectively. The wavelength tuning range of the fiber laser was over 14.2 nm by varying the FBG temperature from 25  $\,^{\circ}$ C to 1000  $\,^{\circ}$ C.

# II. EXPERIMENTAL SETUP

The schematic diagram of the ML fiber laser is shown in Fig. 1 (a). A 980 nm laser diode with a maximal power of 300 mW was used as the pump source. The pump laser was coupled to a

2 m Er-doped fiber (ESF-7/125, Nufern) gain medium by a wavelength division multiplexer (WDM<sub>1</sub>), then passed through the polarization controller (PC<sub>1</sub>). A NOLM was inserted in the ring cavity, which was constructed by an optical coupler (OC<sub>1</sub>) with 40/60 power splitting ratio, a polarization controller (PC<sub>2</sub>) and a loop of single-mode fiber (SMF-28, Corning). Dispersion parameters of the ESF-7/125 fiber and the SMF-28 fiber are 16 ps/km nm and 18 ps/km nm at 1550 nm, respectively. Hence, cavity dispersions were always negative and the fiber laser was a conventional soliton system. When the signal light is sufficient intense, a differential phase shift arising from the intensity mismatch of the counterpropagating beams in the NOLM will accumulate due to the Kerr effect of the fiber. When the phase shift was not greater than  $\pi$ , NOLM can act as a fast SA for producing mode-locking or Q-switching. An FBG was used as the wavelength selection element in the laser cavity. The left hand side of the FBG was connected to No. 2 port of the optical circulator, while its right hand side was beveled to eliminate the interference of the reflected light of the idle end. The laser was coupled out of the cavity by OC2 with 10/90 power splitting ratio. Ninety percent of the light was return to cavity again, and the remaining was sent out of the cavity. The output power and spectrum were measured by a power meter and an optical spectral analyzer (OSA, AQ6370C, Yokogawa Inc.), respectively. The pulse duration was detected by a commercial intensity autocorrelator (FR-103WS, Femtochrome Research Inc.). The pulse trains were characterized by a digital storage oscilloscope (20 GHz sampling scope, DSO9104A, Agilent Technologies Inc.) and a radio frequency (RF) spectrum analyzer (N9000A, Keysight Inc.). An optical isolator was inserted in the cavity to prevent the reflected light and ensure unidirectional propagation.

The FBG was fabricated by 50-fs laser pulses generated by an amplified Ti: sapphire laser (Libra-USP-HE, Coherent, USA) at a center wavelength of 800 nm and a repetition rate of 1 kHz with a Gaussian spatial profile. The Gaussian beam was focused by a cylindrical lens with a focal length of 25 mm and then passed through a zero-order nulled phase mask with period  $\Lambda_{\rm m}{=}2.142~\mu{\rm m}$  into the fiber core. In order to form Type II FBG structures, the distance between the fiber and phase mask was set to less than 1 mm to produce a multiple-beam interference pattern, which has a higher intensity than that generated by pure two-beam interference [20]. The FBG was formed at a laser power of 750 mW using the interval exposure mode, which can suppress the influence of thermal effects [25]. The exposure time and the interval time were 0.1 s and 5 s, respectively.

For realizing stable mode-locking, NOLM length is usually several soliton periods [27], while the amplifier must be shorter than 0.5 soliton periods [26]. The initial NOLM length (fiber pigtails) was about 5 m, while the initial amplifier loop length was about 9.8 m including both 2 m Er-doped fiber and 7.8 m SMF-28 fiber used for PC<sub>1</sub> and element fiber pigtails. The NOLM and amplifier loop lengths were optimized by adding SMF-28 fiber and monitoring fiber laser output. Firstly, the NOLM length was optimized in a step of 50 m. It started mode-locking when NOLM length was about 155 m, but its pulse duration dramatically broadened to a few nanoseconds for NOLM length longer than 305 m, which may be due to the NOLM introduced phase shift has been greater than  $\pi$  [27]. The NOLM length was chosen about 205 m. Then, the amplifier

loop length was optimized. Figure 1(b) shows the variation in pulse energy at different SMF-28 fiber lengths. As the length of SMF-28 fiber in the amplifier loop increased, both output power and pulse energy of the fiber laser increased, while its repetition rate decreased. When the SMF-28 fiber length was longer than 55 m, the fiber laser cannot be mode-locked. Considering the pulse energy and stability of the fiber laser, SMF-28 fiber length in amplifier loop was chosen about 29.8 m. Hence, the ML fiber laser cavity length was about 236.8 m.

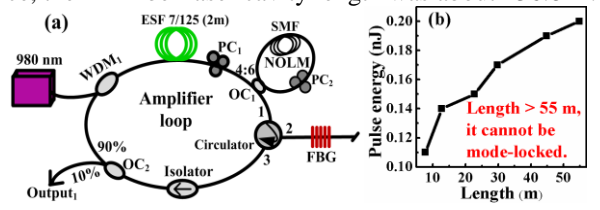


Fig. 1. (a) Schematic diagram of the ML fiber laser. WDM: wavelength division multiplexer (WDM<sub>1</sub>); OC: optical coupler (OC<sub>1</sub>, OC<sub>2</sub>); ESF 7/125: Erbium-doped fiber; PC: polarization controller (PC<sub>1</sub>, PC<sub>2</sub>). (b) Variation in pulse energy at different SMF-28 fiber lengths in the amplifier loop.

# III. RESULTS AND DISCUSSION

The spectrum of the FS laser-inscribed FBG is shown in Fig. 2(a). The peak wavelength and the spectral FWHM of the FBG were 1548.0 nm and 1.0 nm at 25 °C, respectively. The mode-locking of the fiber laser was achieved with a threshold of about 200 mW. Figure 2(a) also shows the output spectrum of the ML fiber laser at a pump power of 300 mW. The peak wavelength of the output spectrum of the fiber laser was 1547.9 nm with a spectral FWHM of 0.90 nm at 25 °C. The output power of the fiber laser was measured to be about 0.15 mW. However, this power was lower than that required by the autocorrelator for measuring, therefore output pulses of the ML fiber laser were amplified firstly for measuring pulse duration. Figure 2(b) shows the schematic diagram of the amplifier. The output pulses of the ML fiber laser were coupled to a 1 m long Er-doped fiber (ESF-7/125, Nufern) through the WDM<sub>2</sub> as seed pulses. The Er-doped fiber was used as gain medium pumped by a 980 nm laser diode. The WDM3 was used to couple amplified laser pulses out of the amplifier. The whole length of the amplifier including SMF-28 fiber and ESF-7/125 fiber from the fiber laser output to autocorrelator was about 5.5 m. In future work, the output power of the ML fiber laser may also be enhanced by optimizing power splitting ratios of  $OC_2$  and  $OC_1$ , lengths of active fiber and NOLM, FBG reflectivity et al.

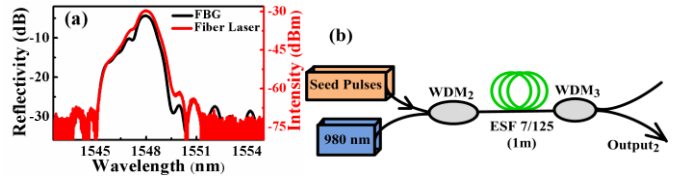


Fig. 2. (a) Reflection spectrum of the FBG and the output spectrum of the ML fiber laser at a pump power of 300~mW. (b) Schematic diagram of the amplifier.

The normalized spectra of both seed pulses at the 300 mW pump power and the amplified pulses at the 600 mW pump power are plotted in Fig. 3(a). It can be seen that the output spectra of both seed and amplified pulses are almost completely overlap. The spectral peak wavelengths and the spectral FWHMs of both seed pulses and amplified pulses were 1547.9 nm and 0.90 nm at 25 °C, respectively. The Fourier-limited pulse duration of the fiber laser was calculated to be about 2.80

ps by assuming sech<sup>2</sup> pulse shape. The measured autocorrelation trace of amplified pulses at a pump power of 600 mW is plotted in Fig. 3(b). The pulse duration of the amplified pulses was about 3.10 ps by assuming sech<sup>2</sup> pulse shape, and time bandwidth product (TBP) was 0.35. It implies the pulse duration of amplified pulses is very close to the Fourier-limited pulse duration. The influence of pump power of the amplifier on its output pulse duration was studied. Variation in pulse duration at different pump powers is shown in Fig. 3(c). The average pulse duration of amplifier output pulses was calculated to be 2.94 ps with a standard deviation of 0.15 ps when the pump power of the amplifier was set between 300 mW and 700 mW. It means that the pump power of the amplifier has little influence on its output pulse duration. Hence, it is reasonable to consider that the pulse duration was only affected by the group delay dispersion of the amplifier after pass through the amplifier. The dispersion introduced by the amplifier including SMF-28 fiber and ESF-7/125 fiber was calculated to be about -0.12 ps<sup>2</sup>. It means the influence of group delay dispersion introduced by amplifier on the output pulse duration of the fiber laser could be neglected. Hence, the pulse duration of the fiber laser can be seen close to the average pulse duration of about 2.94 ps with a corresponding TBP of 0.32.

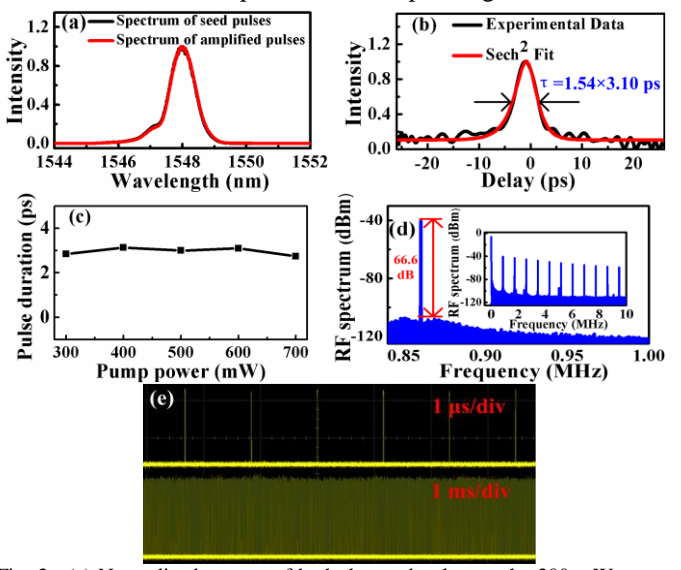


Fig. 3. (a) Normalized spectra of both the seed pulses at the 300 mW pump power and output pulses of the amplifier at the 600 mW pump power. (b). The corresponding autocorrelation trace. (c) Variation in pulse duration at different pump powers of amplifier. Black squares represent the recorded data. (d) The corresponding RF spectrum at 860.5 kHz with a RBW of 1 Hz. Inset: RF spectrum with RBW of 100 Hz. (e) Typical pulse trains.

Figure 3(e) shows typical pulse trains for the amplifier. The repetition rate was measured to be 860.5 kHz. The long range of temporal trace can confirm the stable mode-locking operation of the fiber laser operated without Q-switching instability. The measured RF spectra with a 1 Hz resolution bandwidth (RBW) and a 100 Hz RBW of the amplified ML pulses are shown in Fig. 3(d) and the inset, respectively. The RF spectrum at 860.5 kHz had a signal-to-noise ratio higher than 66.6 dB. The pulse peak power of the fiber laser was calculated to be 56.2 W at 300 mW pump power. Such a low repetition rate ML fiber laser can be directly used as seed source for ultrafast amplifiers and needs no repetition frequency reduction.

The tunability of the FBG-based ML fiber laser was characterized by placing the FBG loosely in a tube furnace that

can be operated from 25 °C to 1200 °C. The fabricated FBG was firstly annealed at 1100 °C for 10 min, and then heated from 300 °C to 1100 °C in steps of 100 °C for 30 min at each temperature. The evolution of FBG reflectivity at different temperatures is shown in Fig. 4(a). It shows that the FBG has good stability at 1000 °C but degrades at temperature above 1000 °C, which was similar as reported in [22]. The pre-annealing at 1100 °C could make FBG quickly reach stable state at 1000 °C. In addition, the silica fiber had no increase in loss but loose almost all of its mechanical strength. This problem could be overcome by using SMF-28 fiber with larger cladding [22]. The inset of Fig. 4(a) shows variations in the fiber laser peak wavelength and intensity at 1000 °C with time before and after annealing at 1100 °C, respectively. The fiber laser peak wavelength was clearly red-shifted and the intensity was continuous decline as time increasing at 1000 ℃ before annealing. Both the peak wavelength and intensity of the fiber laser became stable after annealing. That is, the stability of the ML fiber laser at 1000 °C was greatly improved after annealing the FBG at 1100 ℃. Figure 4(b) shows normalized fiber laser output spectra before and after annealing. The output spectra of the fiber laser before and after annealing were almost the same and both FWHMs of spectra were about 0.90 nm except the weak side band was eliminated after annealing. It means that the pulse duration has nearly no change before and after annealing the FBG.

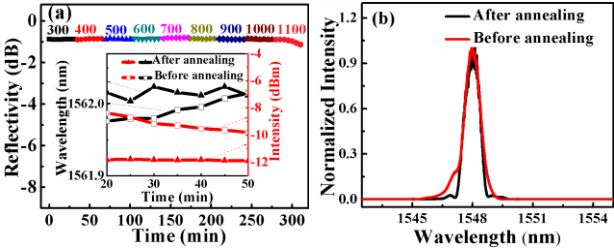


Fig. 4. (a) Variation in FBG reflectivity at different temperatures. Inset: Variations in the fiber laser peak wavelength and intensity at 1000 ℃ before and after FBG annealing. (b) Normalized fiber laser output spectra before and after FBG annealing.

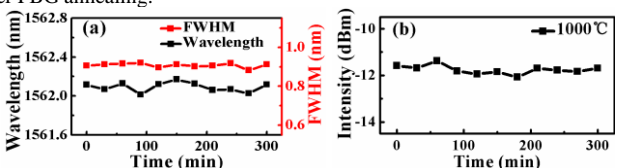


Fig. 5. (a) Variations in the peak wavelength and the spectral FWHM of the fiber laser with the holding time when the tube furnace set at 1000  $^{\circ}$ C. (b)Variation in intensity of the fiber laser with the holding time at 1000  $^{\circ}$ C.

Next, we tested the long-term thermal stability of the fiber laser by putting the FBG in tube furnace which was set at 1000 °C with the holding time of 300 min. Variations in the peak wavelength and the spectral FWHM of the fiber laser with the holding time at 1000 °C are shown in Fig. 5(a). The peak wavelength and the spectral FWHM were 1562.1 nm with a standard deviation of 0.05 nm and 0.90 nm with a standard deviation of 0.01 nm at 1000 °C, respectively. Figure 5(b) shows the variation in the fiber laser intensity with the holding time at 1000 °C. The intensity of the fiber laser only showed small fluctuations of less than 0.70 dB at 1000 °C. The above results imply that the ML fiber laser has a long-term stability for FBG temperature not above 1000 °C.

The behaviors of the wavelength tuning properties of the ML fiber laser were tested in the heating and cooling processes,

respectively. The temperature of the tube furnace was increased from 25 °C to 1000 °C and then decreased to 25 °C in steps of 100 °C for 60 min at each temperature. Figure 6(a) shows the fiber laser output spectra at different temperatures during the heating process. The peak wavelength of the fiber laser increased from 1547.9 nm to 1562.1 nm when the temperature increased from 25 °C to 1000 °C. The spectral profiles at different temperatures were basically coincident. Figure 6(b) shows the fiber laser peak wavelength as a function of temperature from 300 ℃ to 1000 ℃ for heating and cooling processes. Solid curves represent their linear fit ( $R^2 = 99.9\%$ ). Curves of wavelength vs. temperature for cooling and heating are almost completely overlap, which means the fiber laser peak wavelengths have a good repeatability when changing the FBG temperature. The above results imply that the ML fiber laser can stably work as a wavelength-tunable ultrafast laser with a tuning range of over 14.2 nm. The tuning range may be further increased by decreasing FBG temperature to below zero degree or coating FBG with metal to increase its temperature sensitivity. In addition, the ML fiber laser can also work as a high temperature sensor with the maximal sensing temperature up to 1000 ℃ with a sensing sensitivity of 16.1 pm/ ℃ from 300 ℃ to 1000 ℃.

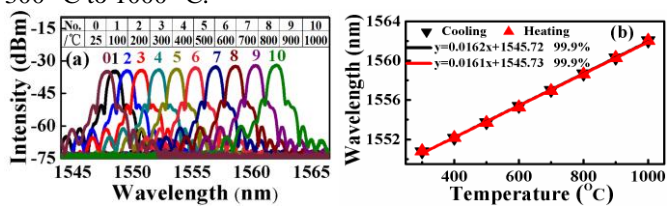


Fig. 6. (a) Spectra at different temperatures during the heating process. (b) The peak wavelength of the wavelength-tunable ML fiber laser as a function of temperature from 300  $\,^{\circ}$ C to 1000  $\,^{\circ}$ C. Solid curves represent the linear fit.

## IV. CONCLUSION

We developed a wide-range wavelength-tunable ML fiber laser based on the FS laser-inscribed FBG as the wavelength selection element and the NOLM as the SA. Its spectral FWHM was 0.90 nm at 25  $^{\circ}$ C. The pulse duration of the fiber laser was about 2.94 ps by assuming sech² pulse shape. The repetition rate was 860.5 kHz. The wavelength tuning range of the fiber laser achieved 14.2 nm by varying the FBG temperature from 25  $^{\circ}$ C to 1000  $^{\circ}$ C. This ML fiber laser may also be used as light source for high-temperature FBG sensing.

## REFERENCES

- [1] C. Dorrer, D. C. Kilper, H.R. Stuart, G. Raybon, and M.G. Raymer, "Linear Optical Sampling," *IEEE Photon. Technol. Lett.*, vol. 15, no. 12, p. 1746-1748, Dec. 2003.
- [2] F. Montserrat, A. Diego, and L. Manuel, "Optimization of the Available Spectrum of a WDM Sensors Network Using a Mode-Locked Laser," J. Lightwave Technol., vol. 33, no. 22, p. 4627-4631, Nov. 2015.
- [3] C. Xu, and F.W. Wise, "Recent advances in fibre lasers for nonlinear microscopy," *Nature Photon.*, vol. 7, p. 875-883, Nov. 2013.
- [4] H. Sotobayashi, J. T. Gopinath, E. M. Koontz, L. A. Kolodziejski, and E. P. Ippen, "Wavelength tunable passively mode-locked bismuth oxide-based erbium-doped fiber laser," *Opt. Commun.*, vol. 237, p. 399-403, Oct. 2004.
- [5] Z. Sun, D. Popa, T. Hasan, F. Torrisi, F. Wang, E. J. R. Kelleher, J. C. Travers, V. Nicolosi, and A. C. Ferrari, "A Stable, Wideband Tunable, Near Transform-Limited, Graphene-Mode-Locked, Ultrafast Laser," *Opt. Lett.*, vol. 3, no. 9, p. 653-660, 2010.
- [6] N. K. Chen, J. W. Lin, F. Z. Liu, and S. K. Liaw, "Wavelength-Tunable Er<sup>3+</sup>-Doped fs Mode-Locked Fiber Laser Using Short-Pass Edge Filters," *IEEE Photon. Technol. Lett.*, vol. 22, no. 10, p. 700-702, May 2010.

- [7] M. Li, X. Zou, J. Qiu, W. Li, and W. Jian, "Tunable Multi-wavelength Dissipative Soliton Generation in an Yb-doped Fiber Laser Based on SESAM and Lyot-Sagnac Filter," OECC, OSA, 2015.
- [8] B. I. Escamilla, O. Pottiez, J. W. Haus, E. A. Kuzin, M. B. Jiménez, and A. F. Rosas, "Wavelength-tunable picosecond pulses from a passively mode-locked figure-eight Erbium-doped fiber laser with a Sagnac fiber filter," J. Eur. Opt. Soc-Rapid., vol. 3, p. 08036, 2008.
- [9] S. M. Zhang, Q. S. Meng, and G. Z. Zhao, "All-fiber wavelength tunable passively mode-locked erbium-doped ring laser," *Eur. Phys. J. D.*, vol. 60, p. 383-387, 2010.
- [10] D. P Zhou, L. Wei, B. Dong, and W. Liu, "Tunable Passively Q-switched Erbium-Doped Fiber Laser with Carbon Nanotubes as a Saturable Absorber," *IEEE Photon. Technol. Lett.*, vol. 22, no. 1, p. 9-11, Jan. 2010.
- [11] I. A. Litago, D. Leandro, M. Á. Quintela, R. A. Pérez-Herrera, M. López-Amo, and J. M. López-Higuera, "Tunable SESAM-Based Mode-Locked Soliton Fiber Laser in Linear Cavity by Axial-Strain Applied to an FBG," J. Lightwave Technol., vol. 35, no. 23, p. 5003-5009, Dec. 2017.
- [12] S. Huang, Y. Wang, P. Yan, J. Zhao, H. Li, and R. Liu, "Tunable and switchable multi-wavelength dissipative soliton generation in a graphene oxide mode-locked Yb-doped fiber laser," *Opt. Express.*, vol. 22, no. 10, p. 11417-11426, May 2014.
- [13] B. Lu, C. Zou, Q. Huang, Z. Yan, Z. Xing, M. A. Araimi, A. Rozhin, K. Zhou, L. Zhang, and C. Mou, "Widely Wavelength-Tunable Mode-Locked Fiber Laser Based on a 45 °Tilted Fiber Grating and Polarization Maintaining Fiber," *J. Lightwave Technol.*, vol. 37, no. 14, p. 3571-3578, Jul. 2019.
- [14] Y. Nakazaki, and S. Yamashita, "Fast and wide tuning range wavelength-swept fiber laser based on dispersion tuning and its application to dynamic FBG sensing," *Opt. Express.*, vol. 17, no. 10, p. 8310-8318, May 2009.
- [15] A. D. Kersey, T. A. Berkoff, and W. W. Morey, "Multiplexed fiber Bragg grating strain-sensor system with a fiber Fabry-Perot wavelength filter," *Opt. Lett.*, vol. 18, no. 16, p. 1370-1372, Aug. 1993.
- [16] J. Jung, H. Nam, B. Lee, J. O. Byun, and N. S. Kim, "Fiber Bragg grating temperature sensor with controllable sensitivity," *Appl. Optics.*, vol. 38, no. 13, p. 2752-2754, May 1999.
- [17] T. Wang, Z. Yan, C. Mou, Z. Liu, Y. Liu, K. Zhou, and L. Zhang, "Narrow bandwidth passively mode locked picosecond Erbium doped fiber laser using a 45° tilted fiber grating device," *Opt. Express.*, vol. 25, no. 14, p. 16708-16714, Jul. 2017.
- [18] Y. Shen, Y. Qiu, B. Wu, W. Zhao, S. Chen, T. Sun, and K. T. V. Grattan, "Short cavity single frequency fiber laser for in-situ sensing applications over a wide temperature range," *Opt. Express.*, vol. 15, no. 2, p. 363-370, Jan. 2007.
- [19] J. Thomas, E. Wikszak, T. Clausnitzer, U. Fuchs, U. Zeitner, S. Nolte, and A. Tünnermann, "Inscription of fiber Bragg gratings with femtosecond pulses using a phase mask scanning technique," Appl. Phys. A., vol. 86, p. 153-157, 2007.
- [20] S. J. Mihailov, C. W. Smelser, D. Grobnic, R. B. Walker, P. Lu, H. Ding, and J. Unruh, "Bragg gratings written in All-SiO<sub>2</sub> and Ge-Doped core fibers with 800-nm femtosecond radiation and a phase mask," *J. Lightwave Technol.*, vol. 22, no. 1, p. 94-100, Jan. 2004.
- [21] Y. Du, T. Chen, Y. Zhang, R. Wang, H. Cao, and K. Li, "Fabrication of phase-shifted fiber Bragg grating by femtosecond laser shield method," *IEEE Photon. Technol. Lett.*, vol. 29, no. 24, p. 2143-2146, Dec. 2017.
- [22] S J. Mihailov, "Femtosecond Laser-Inscribed Fiber Bragg Gratings for Sensing Applications," Opto-Mechanical Fiber Optic Sensors, p. 137-174, 2018
- [23] C. Liao, Y. Li, D. N. Wang, T. Sun, and K. T. V. Grattan, "Morphology and thermal stability of fiber Bragg gratings for sensor applications written in H<sub>2</sub>-free and H<sub>2</sub>-loaded fibers by femtosecond laser," *IEEE Sens. J.*, vol. 10, no. 11, p. 1675-1681, Nov. 2010.
- [24] F. Huang, T. Chen, J. Si, X. Pham, and X. Hou, "Fiber laser based on a fiber Bragg grating and its application in high-temperature sensing," *Opt. Commun.*, vol. 452, p. 233-237, May 2019.
- [25] W. Cui, J. Si, T. Chen, F. Yan, F. Chen, and X. Hou, "Suppression of the thermal effects in the femtosecond laser processing of fiber Bragg gratings," *Chin. Phys. Lett.*, vol. 30, no. 10, p. 104207, 2013.
- [26] J. Theimer and J. W. Haus, "Dispersion balanced figure-eight laser," Opt. Commun., vol. 134, p. 161-164, Jan. 1997.
- [27] N. J. Doran and David Wood, "Nonlinear-optical loop mirror," Opt. Lett., vol. 13, no. 1, p. 56-58, 1988.